

CHEMISTRY

A European Journal

A Journal of



Accepted Article

Title: A “Multi-Heavy-Atom” Approach Toward Biphotonic Photosensitizers With Improved Singlet Oxygen Generation Properties

Authors: Galland Margaux, Tangui Le Bahers, Akos Banyasz, Noelle Lascoux, Alain Duperray, Alexei Grichine, Raphael Tripier, Yannick Guyot, Marie Maynadier, Christophe Nguyen, Magali Gary-Bobo, Chantal Andraud, Cyrille Monnereau, and Olivier Maury

This manuscript has been accepted after peer review and appears as an Accepted Article online prior to editing, proofing, and formal publication of the final Version of Record (VoR). This work is currently citable by using the Digital Object Identifier (DOI) given below. The VoR will be published online in Early View as soon as possible and may be different to this Accepted Article as a result of editing. Readers should obtain the VoR from the journal website shown below when it is published to ensure accuracy of information. The authors are responsible for the content of this Accepted Article.

To be cited as: *Chem. Eur. J.* 10.1002/chem.201901047

Link to VoR: <http://dx.doi.org/10.1002/chem.201901047>

Supported by
ACES

WILEY-VCH

A “Multi-Heavy-Atom” Approach Toward Biphotonic Photosensitizers With Improved Singlet Oxygen Generation Properties.

Margaux Galland,^[a] Tangui Le Bahers,^[a] Akos Banyasz,^[a] Noëlle Lascoux,^[a] Alain Duperray,^[b] Alexei Grichine,^[b] Raphaël Tripier,^[c] Yannick Guyot,^[d] Marie Maynadier,^[e] Christophe Nguyen,^[f] Magali Gary-Bobo,^{*[f]} Chantal Andraud,^{*[a]} Cyrille Monnereau,^{*[a]} and Olivier Maury^{*[a]}

Abstract: Two TACN based ligands bearing three picolinate biphotonic antennae were synthesized and their Yb³⁺ and Gd³⁺ complexes isolated. One series differs from the other by the absence (L¹) / presence (L²) of bromine atoms on the antenna backbone offering respectively improved optical and singlet oxygen generation properties. Photophysical properties of the ligands, complexes and micellar suspension in Pluronic were investigated. Complexes exhibit high two-photon absorption cross-section combined either with NIR emission (Yb) or excellent ¹O₂ generation (Gd). The very large inter-system crossing efficiency induced by the combination of bromine atom and heavy rare-earth element was corroborated with theoretical calculations. The ¹O₂ generation properties of L²Gd micellar suspension under two-photon activation leads to tumour cells death introducing the potential of such structures to offer theranostic applications.

Introduction

Since the discovery of Raab and Von Tappenier in the early 1900 that the activation of organic dyes by light could efficiently induce cell death^[1] followed with the identification by Foote of the related singlet oxygen mediated mechanism,^[2] PhotoDynamic Therapy (PDT) has never ceased to be the object of many research endeavours.^[3] Porphyrins have played a major role in that field,^[4] and their use in clinical application

have become a reality following the groundbreaking works of Dougherty in the 1970's.^[5] PDT has experienced a major burst of interest in the last 15 years: on the one hand various recent proofs of principles have indeed illustrated the relevance and benefits of two-photon activation in the framework of PDT;^[6] on the other hand, singlet oxygen photosensitizers have often been a key component in theranostic architectures.^[7]

In that framework, a significant number of molecular engineering works have attempted to substitute porphyrin macrocycle by better suited photosensitizers. In most of these works, strategies aimed at improving Inter-System Crossing (ISC), *i.e.* the transition from the singlet excited state to a more long-lived and thus reactive triple state able to achieve energy transfer to the surrounding triplet oxygen, have relied on the so called “Heavy Atom Effect”.^[8] Briefly, introduction of atoms of high mass number within the molecule enhance spin-orbit coupling effects, which partially releases the spin forbidden nature of the ISC process.^[8d] Halogen substituted extended π -conjugated chromophores^[9] or third row (Ru²⁺, Ir³⁺) transition metal complexes^[10] have been particularly used in that regard.

- [a] Dr. M. Galland, Dr. A. Banyasz, Dr. N. Lascoux, Dr. T. Le Bahers, Dr. C. Andraud, Dr. C. Monnereau, Dr. O. Maury
Laboratoire de Chimie de l'ENS de Lyon
Univ Lyon, ENS de Lyon, CNRS UMR 5182, Université Claude Bernard Lyon 1, F-69342 Lyon, France.
E-mail: chantal.andraud@ens-lyon.fr; cyrille.monnerneau@ens-lyon.fr; olivier.maury@ens-lyon.fr
- [b] Dr. A. Duperray, Dr. A. Grichine
INSERM, U1209, Université Grenoble Alpes, IAB, F-38000, Grenoble, France
- [c] Pr. R. Tripier,
Univ Brest, UMR CNRS-UBO 6521 CEMCA, IBSAM, UFR des Sciences et Techniques, 6 avenue Victor le Gorgeu, C.S. 93837, 29238, Brest, Cedex 3, France.
- [d] Dr. Y. Guyot,
Univ. Lyon, Institut Lumière Matière, UMR 5306 CNRS–Université Claude Bernard Lyon 1, 10 rue Ada Byron, 69622 Villeurbanne Cedex, France.
- [e] C. Nguyen, Dr. M. Gary-Bobo,
Faculté de Pharmacie, Institut de Biomolécules Max Mousseron, UMR 5247 CNRS-UM, 15 Avenue Charles Flahault, 34093 Montpellier Cedex 05, France.
E-Mail: magali.gary-bobo@univ-montp1.fr
- [f] Dr. M. Maynadier,
NanoMedSyn, 34093 Montpellier, France.

Supporting information for this article is given via a link at the end of the document. ((Please delete this text if not appropriate))

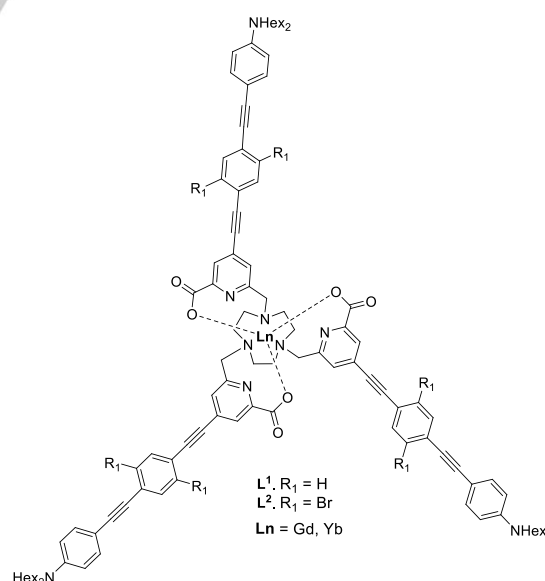


Figure 1. Structure of the lanthanide complexes.

Conversely, in spite of their large atomic mass which ensures efficient ISC, the use of lanthanide complexes as potential PDT

FULL PAPER

WILEY-VCH

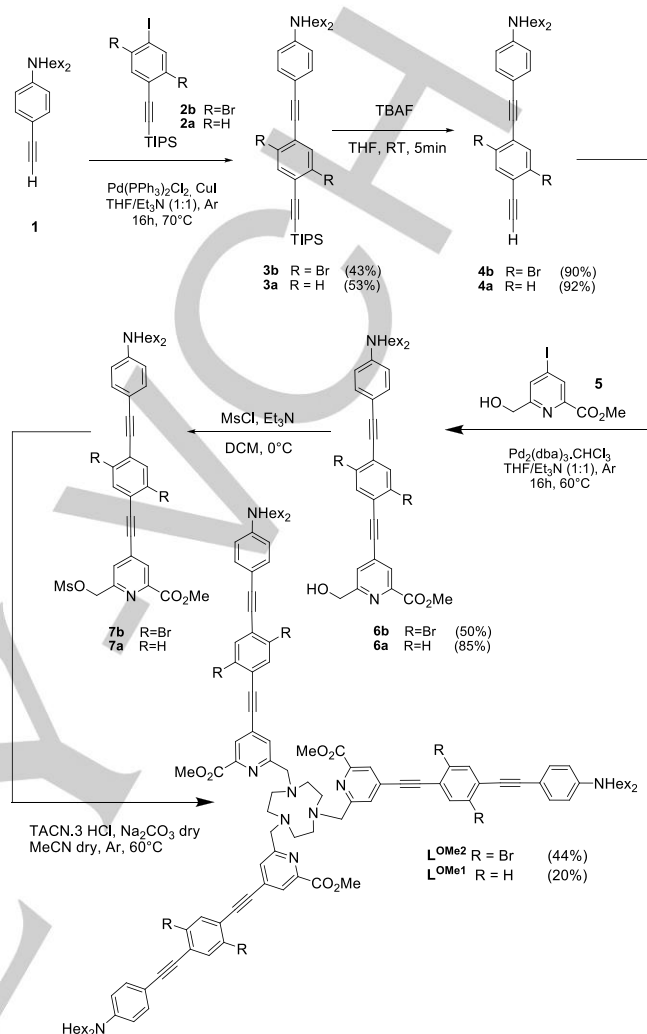
photosensitizers has been relatively less studied to date.^[11] Pioneering works by Sessler and co-workers in the late 90's pointed out the potentialities of texaphyrin lutetium or gadolinium complexes for PDT, one of this complex lutetaphyrin being a clinically used one photon sensitizer.^[11d,e] Several examples described the influence of oxygen as quencher of lanthanide luminescence leading to the design of oxygen sensors^[12] and the competition between lanthanide sensitization and singlet oxygen generation has recently been exemplified on Yb(III) by Faulkner and co-workers using a pyrene antenna.^[13] Recently, the particularly strong heavy atom effect of Gd(III), a non-emissive lanthanide ion has been reported leading to very efficient singlet oxygen generation efficiency (Φ_{Δ} over 80%).^[14] This observation led us to consider that lanthanide complexes may have been overlooked to date particularly in the framework of two-photon PDT, in spite of little matched potential. Indeed the association of their sensitivity to oxygen with the intrinsic features of lanthanide complex, such as long lived luminescence ranging from the visible to the Near Infra-Red (NIR) (Tb^{3+} , Eu^{3+} , Yb^{3+} , Nd^{3+} , Sm^{3+}) or magnetic properties (Gd^{3+} , used in Magnetic Resonance Imaging (IRM) contrast agents) could be of high interest in view of theranostic applications.^[15] In this context, recent works from the groups of Heitz and Tóth reported interesting theranostic bimetallic complex combining two-photon PDT and MRI in which the Gd(III) ion is mainly confined in the role of contrast agent.^[16]

In the present article, and in the framework of ongoing researches dealing with the use of lanthanide complexes for one- and two-photon imaging application,^[12c, 17] we explored the potential of Yb(III) and Gd(III) complexes based on functionalized tris-picolinate 1,4,7-Triazacyclonane (TACN) macrocyclic ligands as photosensitizers. In order to improve their nonlinear optical properties, and render them compatible with two-photon activation, the ligand was functionalized with extended π -conjugated Charge Transfer (CT) antennae featuring or not additional bromine atoms along their backbone (Ligand L^1 and L^2 , Figure 1) known to favor ISC and consequently singlet oxygen generation, when localized at the right position.^[18] We demonstrated a strong synergy for singlet oxygen generation efficiency when combining a bromine substituted ligand to a Gd(III) cation. As a result, a strong enhancement in singlet oxygen generation efficiency is characterized, making our approach introduced herein particularly effective towards the design of improved two-photon photosensitizers with potential utility in theranostics. To illustrate this prospective, incorporation of the Gd^{3+} complex into pluronic micelles was explored, affording nano-objects capable of inducing breast cancer cell death under two-photon excitation.

Results and Discussion

The synthesis of the target ligands $L^{OMe1,2}$ is described in scheme 1. Details about the materials, methodology, synthetic protocol and complete chemical characterization of all intermediates are given in the supporting information. Briefly, both ligands were obtained using a similar convergent methodology: the antennae were prepared using a series of Sonogashira coupling and deprotections of the intermediate silylated alkynes, terminal OH were mesylated and the resulting molecules were involved in a triple nucleophilic substitution on the secondary amines of TACN, to afford the triply functionalized ligands L^{OMe1} and L^{OMe2} after purification by column

chromatography. The methylester functions were then hydrolyzed leading to free ligands $L^{1,2}$ and complexed with the $LnCl_3 \cdot 6H_2O$ salts ($Ln = Gd$ or Yb) using classical reported procedures.^[17b]



Scheme 1. Synthetic procedure for L^{OMe1} and L^{OMe2} .

The photophysical properties of $L^{OMe1,2}$ and their related $LnL^{1,2}$ ($Ln = Yb, Gd$) complexes were studied in diluted dichloromethane (DCM) solution (Figures 2-4, Figure S2,3, and Table 1). The experimental data were systematically compared with theoretical analysis performed on Y(III) model complexes using simplified ligands featuring only one π -conjugated antenna $YL^{1,2}$ (Table S1, Figure 5).^[19] Computational and photophysics details are reported in the supplementary information. As expected, the low energy part of the absorption spectra of the ligands is in all cases dominated by a broad and structureless transition presenting the characteristic features of a Charge Transfer (CT) transition from the strong electro-donating dialkylamino group to the moderate electron withdrawing picolinate moieties (with a strong HOMO-LUMO character).^[16] A second transition is also observed at higher energy that can be assigned to a $^1LE \pi-\pi^*$ transition corresponding to the HOMO-1 to LUMO (figure 5) localized on the central part of the conjugated scaffold. Interestingly, whereas complexation has a little influence on the absorption maxima, the presence of

FULL PAPER

WILEY-VCH

bromine atoms induces a bathochromic shift of ca. 35 nm of the CT transition. This can be ascribed to the electron withdrawing character of the bromine substituent, which increases the CT character of the transition and is also consistent with computations.

Table 1. Photophysical properties of ligands L^{OMe1} , L^{OMe2} and related $LnL^{1,2}$ ($Ln = Yb, Gd$) complexes in DCM solution and $NP^{1,2}$ suspension in PBS buffer at room temperature.

	λ_{abs} (nm)	λ_{em} (nm)	ϵ ($L \cdot mol^{-1} \cdot cm^{-1}$)	$\Phi^{[a]}$ (%)	$\Phi_{\Delta}^{[b]}$ (%)
L^{OMe1}	390	566	66000	24	0
L^{OMe2}	424	600, 1280	117000	9	24
GdL^1	400	615, 1280	92000	2	54
GdL^2	426	624, 1280	79000	1	80
YbL^1	400	580, 980	87000	< 1	0
YbL^2	430	580, 980	85000	< 1	0
NP^1	384	593	-	-	-
NP^2	417	636	-	-	21 ^[c]

[a] luminescence quantum yield is measured in the visible considering only the residual emission of the ligand centered transition with coumarin 153 in MeOH used as a reference ($\lambda_{ex} = 400$ nm, $\Phi_{ref} = 45$ %); [b] phenalenone in DCM used as a reference compound ($\Phi_{\Delta} = 95$ %); [c] measured in water using competitive recombination method with DPAA scavenger (see SI).

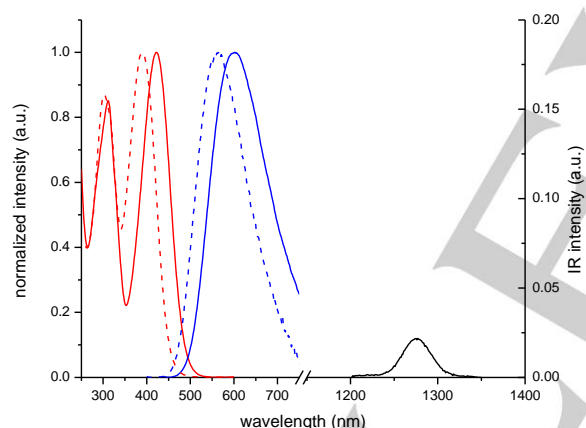


Figure 2. Normalized absorption (red), visible emission (blue) and NIR emission (black) of L^{OMe1} (dashed lines) and L^{OMe2} (straight lines) in DCM at RT ($\lambda_{ex} = 400$ nm).

To confirm this assignment, the amount of charge transferred in this transition could be quantified using the theoretical q_{CT} index based on the integration of the computed electron density variation. As expected an important q_{CT} of 0.6 and 0.7 was computed for non-brominated molecules and for brominated molecules, respectively (Table S1). Qualitatively speaking, the charge transfer character of the transition is also demonstrated by the drawing of the molecular orbitals involved in the first transition, namely the HOMO and the LUMO (Figure 5). The HOMO is mainly localized on the dialkylaniline group while the LUMO is delocalized on central phenyl and pyridine groups, in line with the aforementioned description. The molar extinction coefficients are within experimental error, similar for all studied compounds ca $9.10^4 L \cdot mol^{-1} \cdot cm^{-1}$. All compounds also present a broad, structureless ligand centred emission, which is

characterized by a large Stokes shift (ca $7500 cm^{-1}$) typical for charge transfer transitions. Concerning the ligands, a similar bathochromic effect as for the absorption spectra is observed upon introduction of bromine substituents (L^{OMe1} 566 nm and L^{OMe2} 600 nm, $\Delta\lambda_{em} = 34$ nm). As already observed, complexation by a lanthanide cation (Gd or Yb) results in a significant quenching of the ligand centred emission; the weak residual emission band presents a marginal red-shift as compared to the free ligand. Ligand L^{OMe1} features a moderately high emission quantum efficiency ($\Phi=24$ %). In addition, the introduction of bromine substituents onto the molecule results in a marked quenching of the luminescence (L^{OMe2} $\Phi=9$ %) which, can be assessed to the increased ISC rate in the latter (*vide infra*), in agreement with what has already been observed on a related organic quadrupolar chromophore.^[18]

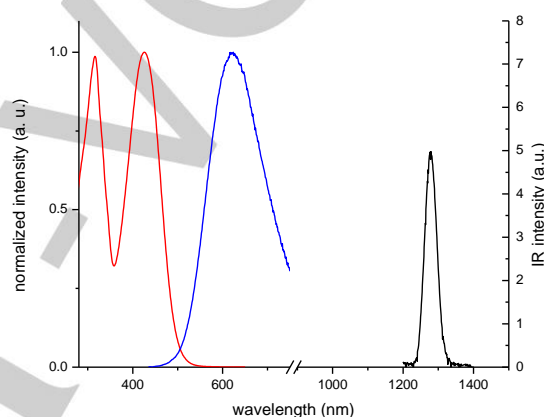


Figure 3. Normalized absorption (red), visible emission (blue) and NIR emission (black) of GdL^2 in DCM at RT ($\lambda_{ex} = 400$ nm).

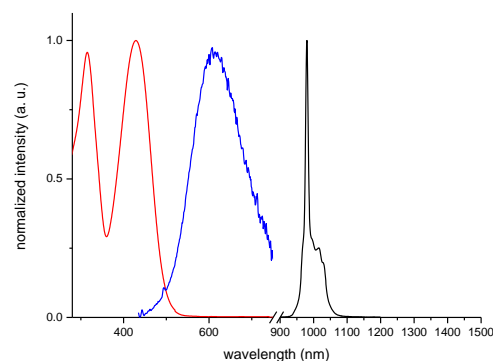


Figure 4. Normalized absorption (red), visible emission (blue) and NIR emission (black) of YbL^2 in DCM at RT ($\lambda_{ex} = 400$ nm).

For the ytterbium complexes $YbL^{1,2}$ the decrease in ligand centred emission is accompanied by the apparition of an intense emission in the NIR at 980 nm, characteristic of the $^2F_{5/2} \rightarrow ^2F_{7/2}$ transition associated with Yb(III). This evolution can be attributed to a very efficient energy transfer between the ligand excited state and the $^2F_{5/2}$ level of ytterbium, via the so-called antenna effect.^[20] The lifetimes of the f-f transition, measured in diluted DCM solution, were found to be 9.3 and 9.7 μs for YbL^1 and

FULL PAPER

WILEY-VCH

YbL^2 , respectively (Figure S4). The lifetimes are almost identical indicating that the emission efficiency of these complexes is rather similar. Since the Yb sensitization can proceed either from the CT or from the triplet excited state,^[20] the influence of the bromine antenna functionalization (favoring the ISC process, hence triplet sensitization) is not apparent on this system.

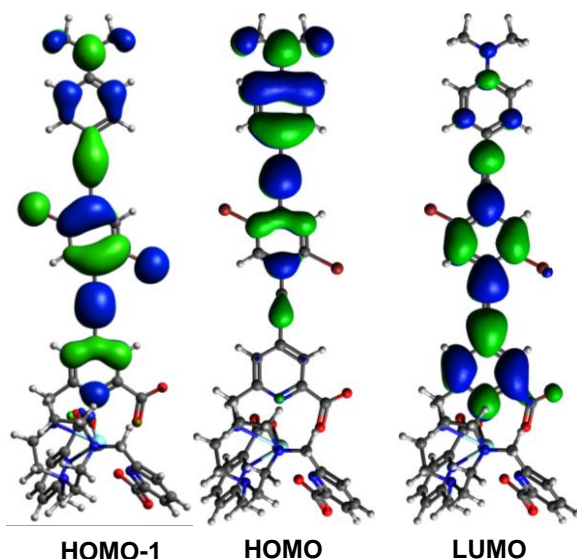


Figure 5. HOMO(-1), HOMO and LUMO orbitals of the YL^2 molecule, involved in the first electronic transition (isocontour 0.02 a.u.).

On the other hand, for the Gd(III) complexes, although no transfer to the lanthanide cation is energetically feasible, the ligand centred emission intensity is however strongly affected by the complexation. This can be ascribed to increased ISC rate resulting from the presence of the heavy Gd cations.^[14] Interestingly, it appears that this quenching of the luminescence is further enhanced upon introduction of halogen substituents. Indeed, while GdL^1 still presents a residual fluorescence quantum yield of ca 2%, it is reduced to less than 1% for GdL^2 (Table 1). Again, this can be put in line with the increased ISC rate that is expected to result from the heavy atom effect of bromine substituents. It is worth noting that, the decrease of fluorescence quantum yield is by itself not a proof of the increased ISC-rate as numerous other non-radiative processes may induce the decrease of the fluorescence. In the following, though, we present the concomitant singlet oxygen generation experiments that strongly support the above-mentioned hypothesis (Table 1).

While the non-substituted ligand L^{OMe1} does not provide any measurable singlet oxygen generation, introduction of bromine substituents (L^{OMe2}) results in a significant improvement in the photosensitizing properties, as singlet oxygen generation quantum efficiency reaches 24%. Similarly, complexation of Gd cation with the halogen free ligand is also seen to efficiently drive the ISC process: GdL^1 presents a singlet oxygen generation efficiency (54%) even higher than that of L^{OMe2} alone. The most important result of this study, however, is achieved upon complexation of the halogen substituted ligand with Gd cation (GdL^2): in the latter case, a synergetic effect of the different heavy atoms on the ISC efficiency can be

unambiguously characterized, which translates into a much improved singlet oxygen generation ability of GdL^2 of 80%.

This evolution drastically differs from that observed in our previous works dealing with halogenated derivatives of purely organic chromophores.^[18] In the latter, we had clearly evidenced that the essential part of the benefits arising from the introduction of bromine substituents along the π -conjugated backbone of the chromophore on the ISC efficiency was obtained after the introduction of a single substituent; additional substitutions only resulted, at best, in a marginal increase of k_{ISC} and Φ_{Δ} , but were mostly inefficient and in some cases even detrimental to the photosensitizing ability of the chromophore.^[18a] Here, opposite conclusions can be drawn, as the singlet oxygen generation efficiency of GdL^2 corresponds, within experimental errors, to the additive effect of the two contributions: bromine substitution and gadolinium complexation. As a consequence, the singlet oxygen generation ability of GdL^2 compares well with that of some of the best photosensitizers reported to date, including clinically used porphyrin derivatives.^[4b] The absence of any singlet oxygen in the corresponding Yb(III) complex can be explained by a much faster intramolecular energy transfer leading to Yb(III) luminescence in regard with the intermolecular collisional energy transfer affording singlet oxygen.^[13, 14b]

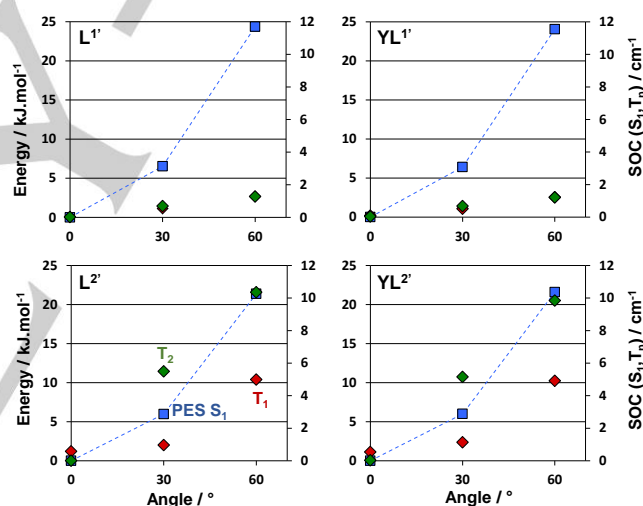


Figure 6. Variation of the potential energy surface (PES) of the S_1 state along the rotation around a triple bond (blue curve and squares). Spin-Orbit Coupling between the S_1 and T_n states computed for each angle of rotation (green symbols T_2 state, red symbol T_1 state).

The DFT and TD-DFT calculations bring an interesting point of view on the mechanism of the ISC. It is well documented in the literature that rotation around triple bond spacers is almost barrierless at the ground state and is more difficult at the excited state.^[18d, 21] This behaviour is also observed on our system, based on the energetic scan along the rotation around the triple bond spacer, computed at the S_1 excited state (the excited CT state). While more difficult than in the ground state, the rotation is still possible at the excited state, with an energy increase of only $\sim 5 \text{ kJ.mol}^{-1}$ for a rotation of 30° . The calculation of the spin-orbit coupling between the S_1 state and T_n states have been performed as a function of the rotation around the triple bound. Only the triplet states lower in energy than the S_1 state were considered, namely the T_1 and T_2 states (Figure S1) and based on the molecular orbitals involved in these states can be ascribed to ^3CT and ^3LE states respectively. Results are given in

FULL PAPER

WILEY-VCH

the Figure 6. It clearly appears that, the flat structure (0° of rotation) undergoes almost no coupling between S_1 state and T_n states. A rotation is necessary to increase notably the spin-orbit coupling between these states. While the increase is modest for non-brominated molecules, it is notably larger for brominated ones. Furthermore, for brominated molecules, the S_1 - T_2 coupling is much larger than the S_1 - T_1 coupling. The rotation around the triple bond cannot explain the increase of ISC induced by the rare-earth element, but is necessary to ISC induction by the bromine substituents.

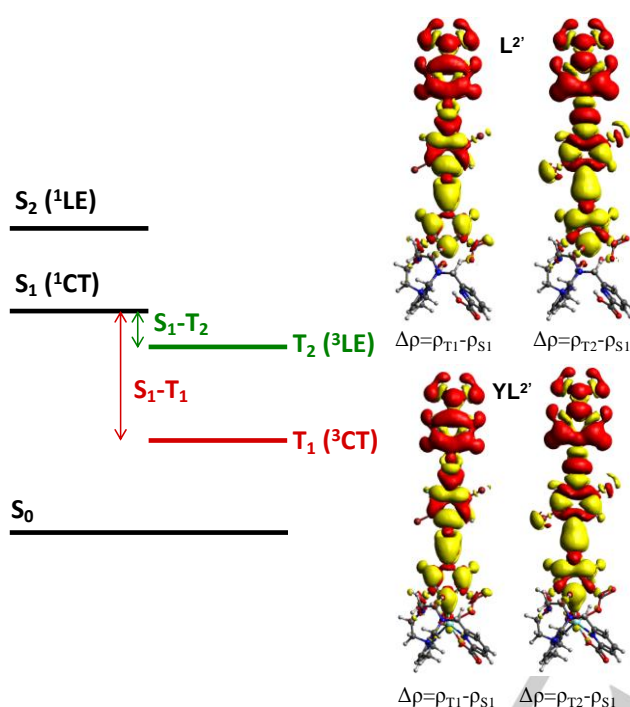


Figure 7. Simplified Perrin-Jablonski diagram (left) and (right) variation of the electron density between the S_1 and the T_n ($n = 1, 2$) states for $L^{2'}$ (top) and $YL^{2'}$. Red and yellow areas correspond to electron increase and depletion regions respectively (isocontour 0.0002 a.u.).

To understand the origin of the larger coupling with the T_2 state, the variation of the electron density between S_1 and T_n states were computed (Figure 7). Both transitions ($S_1 \rightarrow T_1$ and $S_1 \rightarrow T_2$) have a charge transfer character with an increase of the electron density of the aniline group. It means that the T_n states have a less charge-separated character than the parent S_1 state. It appears that the bromine atoms are much more involved in the $S_1 \rightarrow T_2$ transition than in the $S_1 \rightarrow T_1$ transition. Since the bromine atoms have an important contribution to the Spin-Orbit Coupling, it explains why the $S_1 \rightarrow T_2$ coupling is larger than the $S_1 \rightarrow T_1$ one. The spin-orbit coupling exaltation induced by deformations has also been proposed and rationalized in the field of Thermally Activated Delayed Fluorescence (TADF) by Monkman et al.^[22] In addition to this increase of spin-orbit coupling due to the molecular vibrations, Monkman et al. also suggest a mechanism of S_1 - T_1 coupling involving another triplet state. Our computational results prove that the three-states model can be used to compute triplet population for other application such as singlet-oxygen generation. For the rare-earth containing molecules, a slight contribution of the rare-earth element to the variation of the electron density is computed. It highlights that this element is also involved in the transition. We have shown that bromine contribution to the spin-orbit coupling is activated

by a distortion of the molecule (such as the rotation around a triple bond spacer), the rare earth element contribution could also be activated by a deformation, not yet found. Another explanation sometimes proposed in the literature corresponds to an increase of the S_1 - T_1 mixing due to the paramagnetic nature of the Gd^{3+} ion. This phenomenon, first theorized by Tobita et al.^[23] has been assessed on several rare-earth element based complexes.^[24]

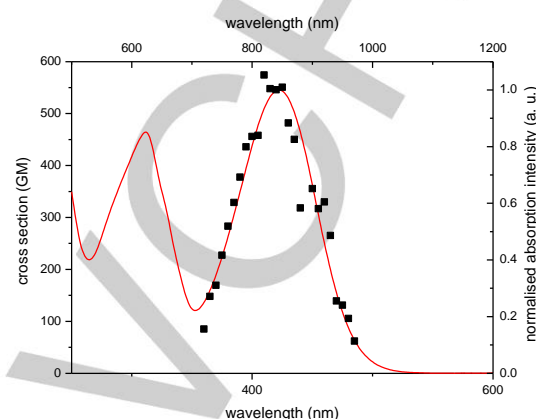


Figure 8. 1P-absorption spectrum of L^{OMe2} in DCM at RT (red line, lower abscissa). Superimposed on this plot is the 2P-absorption measured by TPEF method in DCM in wavelength doubled scale (■, upper abscissa).

Finally, the nonlinear optical properties of the ligand were estimated using the Two-Photon Excited Fluorescence (TPEF) method using a tunable fs-Ti-sapphire source (see supporting information for details). These measurements were only performed on the ligands L^{OMe1} and L^{OMe2} because of a too weak residual visible emission of the related complexes to ensure reliable 2P cross-section measurements by this mean. The two-photon absorption (2PA) spectra of L^{OMe1} and L^{OMe2} are reported in figure S7 and figure 8, respectively. They are found to superimpose perfectly with the main CT transition in the one-photon absorption (1PA) spectra, in good agreement with the non-centrosymmetric character of the molecule. The maximal two-photon absorption cross-section (σ^2) is estimated to 540 GM at 810 nm for L^{OMe2} and 950 GM at 780 nm for L^{OMe1} . This value is in the range of the best 2PA cross-section already described for lanthanide ligand and/or complexes.^[17, 25]

In conclusion of this spectroscopic study, it appears that the “multi-heavy atoms” strategy that consists in combining bromine atoms on the ligand and a complexation with Ln(III) to increase ISC rate leads to the design of a very straightforward singlet oxygen photosensitizer GdL^2 , combining large Φ_A value (80%) with very high one- and two-photon absorption efficiency ($\epsilon \sim 80000 \text{ L.mol}^{-1}.\text{cm}^{-1}$ and $\sigma^2 \sim 540 \text{ GM}$). Keeping in mind that figure-of-merit of a 1P- or 2P-sensitizer is the product $\Phi_A \times \epsilon$ and $\Phi_A \times \sigma^2$, respectively (for GdL^2 $\Phi_A \times \epsilon = 64000 \text{ L.mol}^{-1}.\text{cm}^{-1}$ and $\Phi_A \times \sigma^2 = 430 \text{ GM}$) GdL^2 present real potentiality for practical applications in PDT. In addition, the computational results highlight the importance to have a dynamical point of view on the strength of the spin-orbit coupling that depends not only on the composition of the system (i.e. the presence of heavy atoms) but also on the possibility to undergo geometrical distortions able to remove selection rules associated to spin-orbit coupling.^[18d]

As a consequence of the presence of lipophilic alkyl substituents on their periphery (chosen to ease their spectroscopic study in organic solvents, by alleviating stacking issues) these $GdL^{1,2}$

FULL PAPER

WILEY-VCH

complexes are absolutely not soluble in water nor in any biological media. We thus decided to use a cargo strategy in order to stabilize micellar suspensions of the complexes compatible with such media. To that end, a dispersion using an amphiphilic polymer (Pluronic F127, $n = 100$, $m = 65$, figure 9) has been envisaged, because of the well-known compatibility of this polymer with *in cellulo* PDT, drug delivery or bioimaging applications.^[26] The Pluronic/GdL^{1,2} nanoparticles, noted **NP**^{1,2} are prepared through self-assembly, achieved by adding a phosphate saline buffer (PBS) solution to a THF solution of GdL^{1,2} complexes and Pluronic polymers. After slow evaporation of the THF and filtration on 100 nm pore size filter, a bright orange colloidal suspension in water is obtained. Both particles population, measured by dynamic light scattering present a homogeneous dispersion size centered at 50 nm (Figures 9, S9-10). The spectroscopic properties of the nanoparticles in PBS (Figures S5, S6, Table 1) compare well with their respective parent complexes in DCM indicating that the structure of the complex is preserved in the NPs. The singlet oxygen generation quantum yield cannot be measured in water by relative luminescence measurement because of the very short lifetime of this reactive species in such protic medium. Consequently, the singlet oxygen quantum yield was estimated via a competitive reaction method using dipropionic acid anthracene (DPAA), a fluorescent singlet oxygen scavenger evolving into a nonfluorescent endoperoxide species upon reaction with singlet oxygen.^[27] The comparison of the disappearance kinetic constant of DPAA in the presence of **NP**² suspension or benchmark phenalenone as photosensitizers enable us to estimate the $\Phi_{\Delta}(\text{NP}^2)$ to ca. 21% in water (see SI for details, Figure S7, Table S2).^[28]

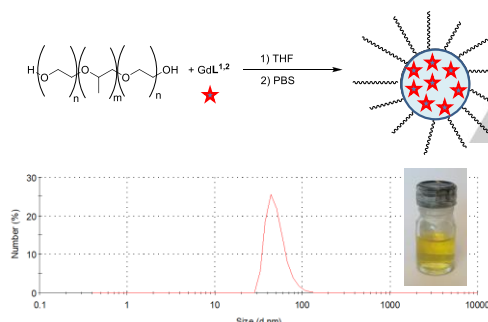


Figure 9. Synthesis of the Pluronic/GdL^{1,2} nanoparticles and picture of the suspension in PBS (top). DLS of **NP**² and two-photon images of living T24 cells stained with **NP**¹ ($\lambda_{\text{ex}} = 800$ nm, bottom).

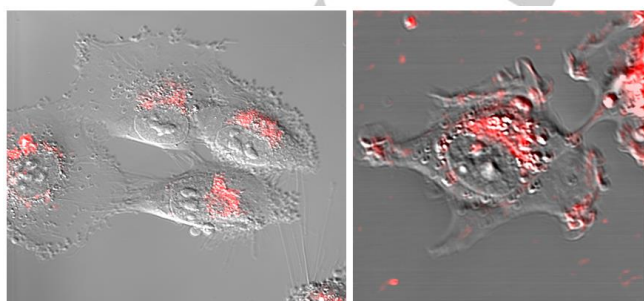


Figure 10. Intracellular distribution of GdL¹ in lived T24 cells after staining with **NP**¹ nanoparticles. Overlay of transmitted light (DIC) imaging and 1P-(left) and 2P-(right) fluorescence microscopy imaging. 1P- and 2P-excitation wavelengths are respectively 405 and 800 nm.

Preliminary tests concerning the behaviour of these NPs *in cellulo* were undertaken using **NP**¹. In spite of the weak residual

emission of GdL¹, live human T24 cancer cells have been stained with **NP**¹ and successfully imaged with one ($\lambda_{\text{ex}} = 405$ nm) or two-photon ($\lambda_{\text{ex}} = 800$ nm) microscopy (Figure 10). The pictures clearly indicate the presence of the emissive species in the endoplasmic reticulum of the cell, indicating that the NPs have successfully transported the lipophilic complex inside the cells. The perinuclear intracellular localization of the compound overlaps well the typical mitochondria-rich region. This proximity (and probable co-localization) would further favour PDT efficiency through apoptosis and other reported anticancer mechanisms.^[29]

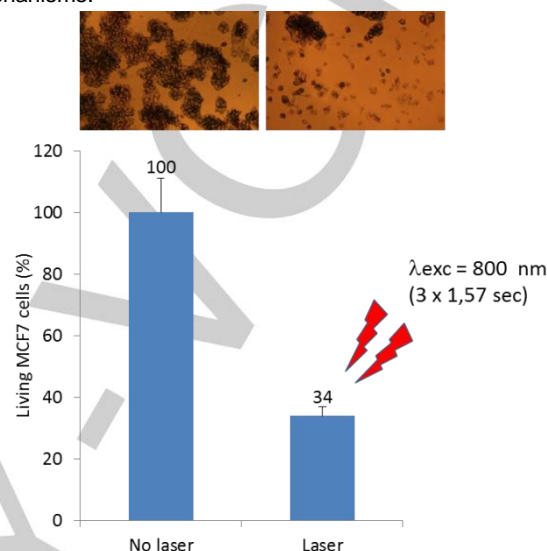


Figure 11. 2P-PDT experiment. MCF-7 cells were incubated with GdL² (30 μM) for 24 h and or not irradiated with a pulsed laser by 3 scans of 1.57 sec at 800 nm (maximal power laser input 3W). Cell survival measurements were done by the MTT assay 48 h after irradiation. (Top) pictures show the difference between non irradiated and irradiated cells after MTT coloration. (Bottom) bar graphs are the results of the quantification. Data are mean values \pm standard deviation from three experiments.

Finally, the photodynamic therapy (PDT) potential of GdL² was performed on human breast cancer cells stained with **NP**² nanoparticles under 2P-excitation (TPE). MCF-7 breast cancer cells were treated with **NP**² (leading to an estimated concentration in GdL² in the medium of 1 and 30 μM , respectively) and submitted or not to a laser irradiation safe for cells (Figures 11 and S11). All controls were done to determine the part of cell death due to the **NP**² treatment followed by irradiation. In fact, non irradiated cells without **NP**², or cells incubated with **NP**² and not irradiated, exhibit no significant cell death in the conditions used here (data not shown). At lower concentration (1 μM), the 2P-PDT effect was not clearly detectable which let us try with a higher concentration (Figure S11). At 30 μM , the combination of **NP**² and 2P-irradiation (3x 1.57 s) clearly induced a strong modification of the cells aspect: the initially clustered cells are completely dispersed in the irradiation area. Furthermore the quantification of cell viability by MTT assay staining only living cells, demonstrated 66% of cell death. This strong effect obtained at 30 μM concentration, after only 3 x 1.57 seconds of irradiation using a medium power laser (Carl Zeiss 10x/0.3 EC Plan-Neofluar, laser power input 3W), demonstrates the robustness of the 2P-PDT potential of GdL². We attribute this high efficiency to the combination of the high two-photon cross-section and the large singlet oxygen generation quantum yield of this probe, as shown above.

FULL PAPER

WILEY-VCH

Conclusions

In this article, we showed that coordination of a lanthanide heavy atom to organic ligands could be used to dramatically improve its singlet oxygen photosensitization efficiency, when no energy transfer to the lanthanide is thermodynamically allowed ($\text{Ln} = \text{Gd}$). Such complexes combine high TPA cross-section, alongside with excellent singlet oxygen generation properties in the range of the best two-photon sensitizer reported to date.^[30] Theoretical calculations helped rationalizing the mechanism associated to this very large ISC efficiency. It was evidenced that (i) ISC preferentially occurs from the S_1 to the T_2 rather than the T_1 ; (ii) it requires a lowering in the ligand symmetry, through distortion of the alkyne bridge. On a more applicative point of view, we showed that stabilization of pluronic nano-suspension of the photosensitizer in physiological medium was possible, and that the resulting suspension was effective in generating singlet oxygen in physiological medium upon photo-irradiation. Finally incubation of this suspension in cell cultures resulted in efficient internalization of the PS within the cell, and the incubated PS could be excited by two-photon activation to efficiently mediate cell death.

Finally, this work opens new potentialities for theranostic applications, for the design of gadolinium complexes as a dual MRI and 2P-PDT probe (after modifications of the ligand structure). This approach is currently under investigation in our groups.

Acknowledgements

Author thanks Dr. Y. Bretonnière and Dr. M. Rémond for their help in the preparation of Pluronic nanoparticles. The authors are grateful to ANR (SADAM ANR-16-CE07-0015-01) for financial support. IAB platform was co-funded thanks to grants of "Association pour la Recherche sur le Cancer" (ARC, Villejuif, France), "Ligue Contre le Cancer" (LCC Ise`re/Arde`che) and the CPER program. The authors thank C. Chamot and the PLATIM Imaging and Microscopy platform for the access to the femtosecond laser system. We thank MRI (Montpellier RIO Imaging platform) for confocal imaging facilities. Dr. T. Le Bahers thanks the "Pole Scientifique de Modélisation Numérique (PSMN)" for its computational resources.

Keywords: Gadolinium • Photodynamic therapy • Intersystem crossing • Two-photon microscopy • Lanthanide

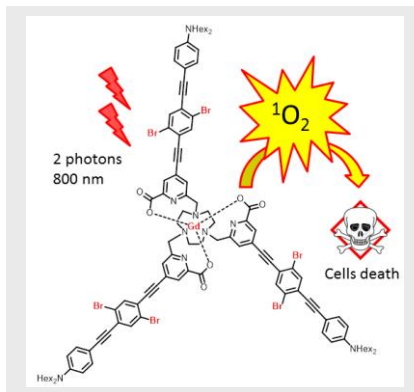
- [1] H. Von Tappenberg, Muench Med Wochenschr **1903**, 47, 2042-2044.
- [2] a) C. S. Foote, *Science* **1968**, 162, 963-970; b) C. S. Foote, *Acc. Chem. Res.* **1968**, 1, 104-110.
- [3] a) T. J. Dougherty, C. J. Gomer, B. W. Henderson, G. Jori, D. Kessel, M. Korbelik, J. Moan, Q. Peng, *JNCI: Journal of the National Cancer Institute* **1998**, 90, 889-905; b) D. E. J. G. J. Dolmans, D. Fukumura, R. K. Jain, *Nature Rev. Canc.* **2003**, 3, 380; c) S. B. Brown, E. A. Brown, I. Walker, *The Lancet Oncology* **2004**, 5, 497-508.
- [4] a) R. Bonnett, *Chem. Soc. Rev.* **1995**, 24, 19-33; A. Ormond, H. Freeman, *Materials* **2013**, 6, 817.
- [5] a) T. J. Dougherty, G. B. Grindey, R. Fiel, K. R. Weishaupt, D. G. Boyle, *JNCI: Journal of the National Cancer Institute* **1975**, 55, 115-121; b) T. J. Dougherty, *J. Clin. Laser Med. & Surg.* **2002**, 20, 3-7.
- [6] P. R. Ogilby, *Chem. Soc. Rev.* **2010**, 39, 3181-3209.
- [7] a) P. Couleaud, V. Morosini, C. Frochet, S. Richeter, L. Raehm, J.-O. Durand, *Nanoscale* **2010**, 2, 1083-1095; b) L. B. Josefsen, R. W. Boyle, *Theranostics* **2012**, 2, 916-966.
- [8] a) A. Gorman, J. Killoran, C. O'Shea, T. Kenna, W. M. Gallagher, D. F. O'Shea, *J. Am. Chem. Soc.* **2004**, 126, 10619-10631; b) S. Kim, T. Y. Ohulchanskyy, D. Bharali, Y. Chen, R. K. Pandey, P. N. Prasad, J. Phys. Chem. C **2009**, 113, 12641-12644; c) M. R. Detty, P. B. Merkel, *J. Am. Chem. Soc.* **1990**, 112, 3845-3855; d) I. V. Khudyakov, Y. A. Serebrennikov, N. J. Turro *Chem. Rev.* **1993**, 93, 537-570.
- [9] a) A. Kamkaew, S. H. Lim, H. B. Lee, L. V. Kiew, L. Y. Chung, K. Burgess, *Chem. Soc. Rev.* **2013**, 42, 77-88; b) C. Tang, P. Hu, E. Ma, M. Huang, Q. Zheng, Dyes Pigments **2015**, 117, 7-15; c) Y. Yang, Q. Guo, H. Chen, Z. Zhou, Z. Guo, Z. Shen, *Chem. Comm.* **2013**, 49, 3940-3942; d) C. Cepraga, S. Marotte, E. Ben Daoud, A. Favier, P.-H. Lanoë, C. Monnereau, P. Baldeck, C. Andraud, J. Marvel, M.-T. Charreyre, Y. Leverrier, *Biomacromolecules* **2017**, 18, 4022-4033; e) C. Cepraga, A. Favier, F. Lerouge, P. Alcouffe, C. Chamignon, P.-H. Lanoë, C. Monnereau, S. Marotte, E. Ben Daoud, J. Marvel, Y. Leverrier, C. Andraud, S. Parola, M.-T. Charreyre, *Pol. Chem.* **2016**, 7, 6812-6825.
- [10] a) M. Stephenson, C. Reichardt, M. Pinto, M. Wächter, T. Sainuddin, G. Shi, H. Yin, S. Monro, E. Sampson, B. Dietzek, S. A. McFarland, J. Phys. Chem. A **2014**, 118, 10507-10521; b) D. Maggioni, M. Galli, L. D'Alfonso, D. Inverso, M. V. Dozzi, L. Sironi, M. Iannaccone, M. Colini, P. Ferruti, E. Ranucci, G. D'Alfonso, *Inorg. Chem.* **2015**, 54, 544-553; c) F. Xue, Y. Lu, Z. Zhou, M. Shi, Y. Yan, H. Yang, S. Yang, *Organomet.* **2015**, 34, 73-77; d) L. K. McKenzie, I. V. Sazanovich, E. Bagdaley, M. Bonneau, V. Guerschais, J. A. G. Williams, J. A. Weinstein, H. E. Bryant, *Chem. Eur. J.* **2017**, 23, 234-238; e) H. Huang, B. Yu, P. Zhang, J. Huang, Y. Chen, G. Gasser, L. Ji, H. Chao, *Angew. Chem. Int. Ed.* **2015**, 127, 14255-14258; f) C. Mari, V. Pierroz, S. Ferrari, G. Gasser, *Chem. Sci.* **2015**, 6, 2660-2686; g) E. M. Boreham, L. Jones, A. N. Swinburne, M. Blanchard-Desce, V. Hugues, C. Terryn, F. Miomandre, G. Lemerrier, L. S. Natrajan, *Dalton Trans.* **2015**, 44, 16127-16135; h) N. Z. Knezevic, V. Stojanovic, A. Chaix, E. Bouffard, K. E. Cheikh, A. Morere, M. Maynadier, G. Lemerrier, M. Garcia, M. Gary-Bobo, J.-O. Durand, F. Cunin, *J. Mat. Chem. B* **2016**, 4, 1337-1342.
- [11] a) G.-L. Law, R. Pal, L. O. Palsson, D. Parker, K.-L. Wong, *Chem. Comm.* **2009**, 7321-7323; b) T. Zhang, R. Lan, C.-F. Chan, G.-L. Law, W.-K. Wong, K.-L. Wong *Proc. Nat. Ac. Sci.* **2014**, 111, E5492-E549; c) X.-S. Ke, Y. Ning, J. Tang, J.-Y. Hu, H.-Y. Yin, G.-X. Wang, Z.-S. Yang, J. Jie, K. Liu, Z.-S. Meng, Z. Zhang, H. Su, C. Shu, J.-L. Zhang *Chem. Eur. J.* **2016**, 22, 9676 - 9686; d) T. D. Mody, L. Fu, J. L. Sessler, *Progress Inorg. Chem.* **2001**, 49, 551-598; e) J. L. Sessler, G. Hemmi, T. D. Mody, T. Murai, A. Burrell, S. W. Young, *Acc. Chem. Res.* **1994**, 27, 43-50.
- [12] a) D. Parker, *Coord. Chem. Rev.* **2000**, 205, 109-130; b) R. Hueting, M. Tropicano, S. Faulkner, *RSC Advances* **2014**, 4, 44162-44165; c) M. Soulié, F. Latzko, E. Bourrier, V. Placide, S. J. Butler, R. Pal, J. W. Walton, P. L. Baldeck, B. Le Guennic, C. Andraud, J. M. Zwiir, L. Lamarque, D. Parker, O. Maury *Chem. Eur. J.* **2014**, 20, 8636 - 8646; d) T. J. Sorensen, A. M. Kenwright, S. Faulkner, *Chem. Sci.* **2015**, 6, 2054-2059; e) A. Watkis, R. Hueting, T. J. Sorensen, M. Tropicano, S. Faulkner, *Chem. Commun.* **2015**, 51, 15633-15636.
- [13] J. Lehr, M. Tropicano, P. D. Beer, S. Faulkner, J. J. Davis, *Chem. Comm.* **2015**, 51, 15944-15947
- [14] a) R. Arppe, N. Kofod, A. K. R. Junker, L. G. Nielsen, E. Dallerba, T. J. Sorensen, *Eur. J. Inorg. Chem.* **2017**, 5246-5253; b) M. Galland, F. Riobé, J. Ouyang, N. Saleh, F. Pointillart, V. Dorcet, B. Le Guennic, O. Cadot, J. Crassous, C. Andraud, C. Monnereau, O. Maury *Eur. J. Inorg. Chem.* **2019**, 118-125.
- [15] a) Y. I. Park, H. M. Kim, J. H. Kim, K. C. Moon, B. Yoo, K. T. Lee, N. Lee, Y. Choi, W. Park, D. Ling, K. Na, W. K. Moon, S. H. Choi, H. S. Park, S.-Y. Yoon, Y. D. Suh, S. H. Lee, T. Hyeon, *Adv. Mater.* **2012**, 24, 5755-5761; b) J. Luo, L.-F. Chen, P. Hu, Z.-N. Chen, *Inorg. Chem.* **2014**, 53, 4184-4191; c) Z. Zhu, X. Wang, T. Li, S. Aime, P. J. Sadler, Z. Guo, *Angew. Chem. Int. Ed.* **2014**, 53, 13225-13228; d) C. Truillet, F. Lux, J. Moreau, M. Four, L. Sancey, S. Chevreux, G. Boeuf, P. Perriat, C. Frochet, R. Antoine, P. Dugourd, C. Portefaix, C. Hoeffel, M. Barberi-Heyob, C. Terryn, L. van Gulick, G. Lemerrier, O. Tillement *Dalton Trans.* **2013**, 42, 12410-12420.
- [16] J. Schmitt, V. Heitz, A. Sour, F. Bolze, P. Kessler, L. Flamigni, B. Ventura, C. S. Bonnet, É. Tóth, *Chem. Eur. J.* **2016**, 22, 2775-2786.
- [17] a) N. Hamon, M. Galland, M. Le Fur, A. Roux, A. Duperray, A. Grichine, C. Andraud, B. Le Guennic, M. Beyler, O. Maury, R. Tripiet *Chem.*

- Commun.* **2018**, *54*, 6173 – 6176; b) A.-T. Bui, A. Roux, A. Grichine, A. Duperray, C. Andraud, O. Maury *Chem. Eur. J.* **2018**, *24*, 3408-3412; c) A. T. Bui, M. Beyler, A. Grichine, A. Duperray, J.-C. Mulatier, C. Andraud, R. Tripier, S. Brasselet, O. Maury *Chem. Commun.* **2017**, *53*, 6005-6008; d) A.-T. Bui, A. Grichine, S. Brasselet, A. Duperray, Chantal Andraud, O. Maury *Chem. Eur. J.* **2015**, *21*, 17757-17761; e) A. D'Aléo, A. Bourdolle, S. Bulstein, T. Fauquier, A. Grichine, A. Duperray, P. L. Baldeck, C. Andraud, S. Brasselet, O. Maury *Angew. Chem. Int. Ed.* **2012**, *51*, 6622 – 6625.
- [18] a) P.-H. Lanoe, T. Gallavardin, A. Dupin, O. Maury, P. L. Baldeck, M. Lindgren, C. Monnereau, C. Andraud, *Org. Biomol. Chem.* **2012**, *10*, 6275-6278; b) T. Gallavardin, C. Armagnat, O. Maury, P. L. Baldeck, M. Lindgren, C. Monnereau, C. Andraud, *Chem. Commun.* **2012**, *48*, 1689-1691; c) B. Mettra, Y. Y. Liao, T. Gallavardin, C. Armagnat, D. Pitrat, P. Baldeck, T. Le Bahers, C. Monnereau, C. Andraud, *Phys. Chem. Chem. Phys.* **2018**, *20*, 3768-3783.
- [19] a) K. Sénéchal-David, A. Hemeryck, N. Tancrez, L. Toupet, J.A.G. Williams, I. Ledoux, J. Zyss, A. Boucekkine, J.-P. Guégan, H. Le Bozec, O. Maury *J. Am. Chem. Soc.*, **2006**, *128*, 12243-12255; b) A. Bourdolle, M. Allali, J.-C. Mulatier, B. Le Guennic, J. Zwier, P. L. Baldeck, J.-C.G. Bünzli, C. Andraud, L. Lamarque, O. Maury *Inorg. Chem.* **2011**, *50*, 4987-4999.
- [20] A. D'Aléo, L. Ouahab, C. Andraud, F. Pointillart, O. Maury *Coord. Chem Rev.* **2012**, *256*, 1604-1620.
- [21] a) B. Mettra, F. Appaix, J. Olesiak-Banska, T. Le Bahers, A. Leung, K. Matczyszyn, M. Samoc, B. van der Sanden, C. Monnereau, C. Andraud, *ACS App. Mat. Inter.* **2016**, *8*, 17047-17059; b) B. Mettra, T. Le Bahers, C. Monnereau, C. Andraud, *Dyes Pigm.* **2018**, *159*, 352-366.
- [22] a) J. Gibson, A. P. Monkman, T. J. Penfold *ChemPhysChem* **2016**, *17*, 2956 – 2961. T. J. Penfold, F. B. Dias, A. P. Monkman *Chem. Commun.* **2018**, *54*, 3926
- [23] S. Tobita, M. Arakawa, I. Tanaka *J. Phys. Chem.* **1984**, *88*, 2697-2702.
- [24] S. Tobita, M. Arakawa, I. Tanaka *J. Phys. Chem.* **1985**, *89*, 5649-5654; b) V. V. Volchkov, V. L. Ivanov, B. M. Uzhinov *J. Fluor.* **2010**, *20*, 299-303.
- [25] A. Picot, A. D'Aléo, P.L. Baldeck, C. Andraud, O. Maury *Inorg. Chem.*, **2008**, *47*, 10269-10279
- [26] a) T. Gallavardin, M. Maurin, S. Marotte, T. Simon, A. M. Gabudean, Y. Bretonniere, M. Lindgren, F. Lerouge, P. L. Baldeck, O. Stephan, Y. Leverrier, J. Marvel, S. Parola, O. Maury, C. Andraud, *Photochem. Photobiol. Sci.* **2011**, *10*, 1216-1225; b) B. Li, E. H. Moriyama, F. Li, M. T. Jarvi, C. Allen, B. C. Wilson, *Photochem. Photobiol.* **2007**, *83*, 1505-1512; c) C. Kim, S.-Y. Kim, Y. T. Lim, T. S. Lee, *Macromol. Res.* **2017**, *25*, 572-577; d) J. R. Navarro, F. Lerouge, C. Cepera, G. Micouin, A. Favier, D. Chateau, M.-T. Charreyre, P.-H. Lanoë, C. Monnereau, F. Chaput, *Biomaterials* **2013**, *34*, 8344-8351; e) X. Yan, M. Remond, Z. Zheng, E. Hoibian, C. Soulage, S. Chambert, C. Andraud, B. Van der Sanden, F. Ganachaud, Y. Bretonniere, J. Bernard *ACS Appl. Mater. Interfaces*, **2018**, *10*, 25154–25165.
- [27] X.-D. Wang, Otto S. Wolfbeis *Chem. Soc. Rev.*, **2014**, *43*, 3666–3761.
- [28] E. Gandin, Y. Lion, A. Van De Vorst *Photochem. Photobiol.* **1983**, *37*, 271-278.
- [29] F. Lin, Y.-W. Bao, F.-G. Wu *Molecules*, **2018**, *23*, 3016-3139.
- [30] a) H. A. Collins, M. Khurana, E. H. Moriyama, A. Mariampillai, E. Dahlstedt, M. Balaz, M. K. Kuimova, M. Drobizhev, V. X. D. Yang, D. Phillips, A. Rebane, B. C. Wilson, H. L. Anderson *Nature Photonics*. **2008**, *2*, 420-424; b) L. Beverina, M. Crippa, M. Landenna, R. Ruffo, P. Salice, F. Silvestri, S. Versari, A. Villa, L. Ciaffoni, E. Collini, C. Ferrante, S. Bradamante, C. M. Mari, R. Bozio, G. A. Pagani *J. Am. Chem. Soc.* **2008**, *130*, 1894–1902; c) J. Schmitt, V. Heitz, A. Sour, F. Bolze, H. Ftouni, J. F. Nicoud, L. Flamigni, B. Ventura *Angew. Chem. Int. Ed.* **2015**, *54*, 169–173; d) C.-L. Sun, Q. Liao, T. Li, J. Li, J.-Q. Jiang, Z.-Z. Xu, X.-D. Wang, R. Shen, D.-C. Bai, Q. Wang, S.-X. Zhang, H.-B. Fube, H.-L. Zhang *Chem. Sci.*, **2015**, *6*, 761-769.

Entry for the Table of Contents (Please choose one layout)

Layout 1:

The TACN based gadolinium complex exhibits high two-photon absorption cross-section combined with near-unity $^1\text{O}_2$ generation. The very large inter system crossing efficiency induced by the combination of bromine atom and heavy rare-earth element was corroborated with theoretical calculations. The $^1\text{O}_2$ generation properties of micellar suspensions under two-photon activation lead to tumour cells death introducing the potential of such structures for theranostic applications.



Margaux Galland, Tangui Le Bahers, Akos Banyasz, No lle Lascoux, Alain Duperray, Alexei Grichine, Rapha l Tripier, Yannick Guyot[†] Marie Maynadier[†] Christophe Nguyen, Magali Gary-Bobo,^{*} Chantal Andraud,^{*} Cyrille Monnereau,^{*} Olivier Maury^{*}

Page No. – Page No.

A “Multi-Heavy-Atom” Approach Toward Biphotonic Photosensitizers With Improved Singlet Oxygen Generation Properties.